Pharm Res (2015) 32:1794–1803
DOI 10.1007/s11095-014-1576-z

RESEARCH PAPER

Osteotropic Polypeptide Nanoparticles with Dual hydroxyapatite Binding Properties and Controlled Cisplatin Delivery

Laura de Miguel • Iuliana Popa • Magali Noiray • Eric Caudron • Ludovica Arpinati • Didier Desmaele • Gerardo Cebrián-Torrejón • Antonio Doménech-Carbó • Gilles Ponchel

Received: 30 May 2014 / Accepted: 11 November 2014 / Published online: 12 December 2014

ABSTRACT

Purpose Nanoparticles with prolonged residence time in bone constitute a valuable strategy for bone disease treatments. The aim of this work was to synthesise a simple nanoparticulate system exhibiting both anticancer and hydroxyapatite binding properties for potential bone cancer applications.

Methods The amphiphilic copolymer poly(γ-benzyl-glutamate)-block-poly(glutamic acid) (PBLG-*b*-PGlu) was synthetised by ring opening polymerization and nanoparticles were obtained by a simple nanoprecipitation method. Nanoparticles were characterized in terms of cisplatin interaction, association, and release as well as interaction with hydroxyapatite and their cytoxicity was studied in three prostate cancer cell lines.

Results PBLG-*b*-PGlu nanoparticles of ~50 nm in size were successfully prepared. They could display for the first time dual hydroxyapatite binding and anticancer properties mediated by the PGlu moiety. They could complex cisplatin at a drug loading content of 6.2% (*w/w*). Cisplatin release was triggered by physiological concentrations of chloride ions according to an almost zero order kinetics during 14 days. Simultaneously, these nanoparticles showed *in vitro* hydroxyapatite binding. Finally, they were shown to exert a cytotoxic effect in three prostate cancer cell lines that potentially metastasize to bone.

Conclusions These properties suggest the potential utility of cisplatin-loaded PBLG-*b*-PGlu nanoparticles as carrier systems for the treatment of bone metastases.

KEY WORDS cisplatin · hydroxyapatite · nanoparticles · poly(benzylglutamate) · poly(glutamic acid)

ABBREVIATIONS

AAS	Atomic absorption spectroscopy
BLG-NCA	γ-benzyl-L-glutamate-N-carboxylic anhydride
$CDCl_3$	Deuterated chloroform
CDDP	Cisplatin
DLS	Dynamic light scattering
DMF	Dimethylformamide
DP_n	Degree of polymerization
FTIR	Fourier transform infrared spectroscopy
H NMR	Proton nuclear magnetic resonance
HAP	Hydroxyapatite
ITC	Isothermal titration calorimetry
MTS	([3-(4,5-dimethylthiazol-2-yl)-5-(3-carboxymethoxyphenyl)-2-(4 sulfophenyl)-2H tetrazolium, inner salt)

Electronic supplementary material The online version of this article (doi:10.1007/s11095-014-1576-z) contains supplementary material, which is available to authorized users.

L. de Miguel (✉) • I. Popa • M. Noiray • L. Arpinati • D. Desmaele • G. Ponchel
Institut Galien Paris-Sud, CNRS UMR 8612, Université Paris-Sud, 5 rue Jean Baptiste Clément, 92296 Chatenay-Malabry, France
e-mail: laura.de-miguel@u-psud.fr

L. de Miguel
e-mail: laurademigueltinez@gmail.com

E. Caudron
Hôpital Européen Georges Pompidou (AP-HP), Service de Pharmacie, Paris, France

E. Caudron
Paris Sud Analytical Chemistry Group, School of Pharmacy, Université Paris-Sud, 5 rue Jean Baptiste Clément, Châtenay-Malabry, France

G. Cebrián-Torrejón • A. Doménech-Carbó
Departament de Química Analítica, Facultat de Química, Universitat de València, Dr. Moliner 50, 46100 Burjassot, Valencia, Spain

PBLG-*b*-PGlu	Poly(γ-benzyl-glutamate)-block-poly (glutamic acid)
PBS	Phosphate buffer saline
ROP	Ring opening polymerization
SEC	Size exclusion chromatography
TEM	Transmission Electron Microscopy
TFA	Trifluoroacetic acid

INTRODUCTION

The skeleton is a common metastatic site for many cancers, including prostate cancer, which constitutes the second leading cause of cancer death in men (1). Metastatic bone disease results in metabolic complications and it is associated with a bad prognosis of the disease (2). Conventional chemotherapy is generally poorly efficient because of inadequate biodistribution in the body and lack of specificity of available drugs. Therapeutic alternatives, including surgical removal of metastasis, can only be foreseen in specific situations, prompting the development of efficiently targeted drug delivery systems.

The design of bone targeted drug delivery systems could constitute a valuable strategy in view of enhancing the distribution of anticancer drugs to bone tissues. Different bone targeted drug carriers have been designed, such as drug conjugates, polymeric drug conjugates and nanoparticles (3,4). Nanoparticles have revealed therapeutically interesting for some cancer treatments. Self-assembly of amphiphilic copolymers into nanoparticles has shown to lead to a precise engineering of such delivery systems through the introduction of the different requested functionalities.

Hydroxyapatite (HAP) interaction and binding has been widely used as a mean to confer osteotropicity to targeted delivery systems (5), including polymeric drug conjugates. Acidic oligopeptides have shown hydroxyapatite binding properties (6) and have been used to provide drugs with osteotropicity (7).

Cisplatin is currently used in combined chemotherapy for advanced prostate cancer and has been shown to efficiently coordinate to PGlu (8). However, its biodistribution properties should be improved since it has a very short half life in the bloodstream due to glomerular excretion (9) and its use is limited due to several side effects (9,10). Therefore, much research has been focused on the development of polymeric cisplatin delivery systems (11).

The objective of this work was to prepare multifunctional nanoparticles with dual anticancer and hydroxyapatite binding properties. These nanoparticles are intended to attach to the bone surface so as to constitute drug reservoirs for local release. For this purpose, a PBLG-*b*-PGlu copolymer was synthesised. The use of a single copolymer which could display dual properties was privileged against other more complex approaches due to its simplicity from a pharmacotechnical point of view, which enables an easy scale-up. The experimental conditions leading to an efficient self-assembly of a PBLG-b-PGlu copolymer by a simple nanoprecipitation method were investigated, as well as the possibility to use the hydrophilic PGlu block to impart simultaneously cisplatin complexing properties and hydroxyapatite binding properties to preformed PBLG-*b*-PGlu nanoparticles. Finally, cytotoxicity studies on three prostate cancer cell lines with a high potential of bone metastases (12) were performed.

MATERIALS AND METHODS

Materials

Dimethylformamide (DMF) (99.8%) Extradry Acroseal and cisplatin (CDDP) were purchased from Acros, γ-benzyl-L-glutamate-N-carboxylic anhydride (BLG-NCA) was provided by IsoChem and used as received. Hexylamine (puriss ≥99.5%), trifluoroacetic acid (TFA) (99%), palladium on carbon, deuterated chloroform ($CDCl_3$), blue trypan and double stranded deoxyribonucleic acid sodium salt from salmon testes (ds-DNA) were provided by Sigma Aldrich. Dialysis membranes were purchased from Carlroth, (Spectra Por). One mL microdialyzers used for *in vitro* drug release experiments were bought from Orange Scientific. $PGlu_{3000}$ and $PGlu_{30000}$ were purchased from Alamanda Polymers. PC-3 were kindly provided by the Institut Curie (Paris, France) and LNCaP and DU-145 were obtained from American Type Culture Collection. CellTiter 96® aqueous one solution cell ([3-(4,5-dimethylthiazol-2-yl)-5-(3-carboxymethoxyphenyl)-2-(4 sulfophenyl)-2H-tetrazolium, inner salt) (MTS) proliferation assay was purchased from Promega.

Synthesis of PBLG-*b*-PGlu Copolymer

A poly(γ-benzyl-L-glutamate)-block-poly(glutamic acid) (PBLG-*b*-PGlu) copolymer was synthesized by a modified method previously described (detailed in Supplementary material (SM)) (13). Briefly, the synthetic approach consisted of preparing a hydrophilic PGlu derivate, which was further used as a macroinitiator for the synthesis of the hydrophobic PBLG block by ring opening polymerization (ROP). Briefly, 1.8 g of BLG-NCA mg were dissolved in anhydrous DMF at a concentration of 0.5 M. The solution was stirred for 10 min and the initiator, a DMF solution of hexyl-PGlu at a concentration of 3.1 M, was added with an argon-purged syringe. The solution was stirred at 30°C during 7 days. Then, the mixture was poured into a large excess of cold diethyl ether and the precipitate filtered and dried over vacuum. A second purification step, involving dissolution in tetrahydrofuran/

methanol 75/25 and reprecipitation into cold diethyl ether, filtration and drying over vacuum was made. The evolution of the reaction was controlled by infrared analysis, by checking the disappearance of BLG-NCA bands and the appearance of the PBLG ones. This polymer was analyzed by proton nuclear magnetic resonance (^{1}H NMR) in $CDCl_3$ + 15% TFA and its molar mass was determined by size exclusion chromatography (SEC).

Synthesis of Other PBLG Derivates

PBLG-bnz and PBLG-dansyl were synthesized by ROP of BLG-NCA in the conditions described above using benzylamine and dansylcadaverine respectively as initiators. For the PBLG-dansyl, purification also included a washing step with methanol.

Characterization of PBLG Copolymers

Fourier Transform Infrared Spectroscopy (FTIR)

FTIR spectra of the polymers were performed on a Fourier Transform Perkin-Elmer 1750 spectrometer using the attenuated total reflection system to confirm the absence of NCA auto-polymerization, to follow the evolution of the polymerization reactions and to study the secondary structure of the polymers.

Proton Nuclear Magnetic Resonance (^{1}H NMR)

^{1}H NMR spectra of polymers were recorded on a Bruker AC 300 MHz spectrometer in $CDCl_3$ + 15% TFA for PBLG polymers and in deuterated dymethylsufoxide (DMSO d_6). The role of the TFA is to disrupt α-helix that PBLG polymers adopt in chloroform, rendering them in a random coil conformation (14).

Size Exclusion Chromatography (SEC)

SEC was used to determine the molar mass of PBLG-*b*-PGlu. The SEC system was equipped with two PLgel 5 µm MIXED-D (7,5 mm ID × 30,0 cm L) and a PLgel 5 µm guard column (guard column 7,5 mm ID × 5,0 cm L), a refractive index detector (Jasco 1530-RI) and a UV detector (Jasco 875-UV). DMF with 1 g/L of lithium bromide (LiBr) was used as a diluent at a flow of 0.8 ml/min at 80°C and linear polystyrene samples were used as calibration standards.

Nanoparticle Preparation

PBLG-*b*-PGlu nanoparticles were prepared following a novel nanoprecipitation method. Briefly, 7.5 mg of the PBLG-*b*-PGlu copolymer were dissolved in 2.5 mL of tetrahydrofuran/methanol 75/25 at 40°C at a concentration of 0.1 nM without magnetic stirring. Once dissolved, they were added by dripping to a 5 mL of aqueous solution containing two equivalents of sodium hydroxide (NaOH) per equivalent of COOH and stirred for 10 min. Solvents were eliminated under vacuum in the rotavapor at 40°C. Nanoparticles size and ζ potential were determined by dynamic light scattering (DLS) at 25°C (Zetasizer 4, Malvern Instruments) after dialysis with a SpectraPor membrane (molecular weight cut off 3000 Da) during 24 h to eliminate the NaOH. PBLG-*b*-PGlu nanoparticle size and ζ potential were measured before and after cisplatin association. Nanoparticles were observed by means of a Transmission Electron Microscopy (TEM) at 120 KV (TEM JEOL 1400) with phosphotungstic acid as a negative coloration agent. Measurements of the longitudinal and axial radius of 100 nanoparticles were made on TEM photos using Image J.

PBLG-*b*-PGlu Nanoparticle Interaction With Cisplatin by Isothermal Titration Calorimetry (ITC)

Interaction of PBLG-*b*-PGlu nanoparticles with cisplatin was studied by ITC (Microcal. Inc. USA). The cell was loaded with PBLG-*b*-PGlu nanoparticles at a molar concentration of polymer of 0.042 mM and a molar concentration of COO^- groups of 0.68 mM. The nanoparticle suspension was placed in the measurement cell (approx. 1.3 mL) and stirred at 112 rpm by the syringe, which was filled with an aqueous solution of cisplatin at a concentration of 0.8 mM. The titration of PBLG-*b*-PGlu nanoparticles involved a first injection of 5 µL followed by 27 injections of 10 µL during 20 s each 300 s. Experiments were carried out at 37°C. PBLG-bnz nanoparticles, not containing COO^- groups, were used as a negative control.

Cisplatin Analytical Determination

The content of platinum was measured by atomic absorption spectroscopy (AAS) (Varian® SpectrAA 220Z) as detailed in SM.

Cisplatin Association to PBLG Nanoparticles

Cisplatin was dissolved in water at a concentration of 1 mg/mL and reacted with silver nitrate ($AgNO_3$) in a 1/1 [$AgNO_3$/CDDP] molar ratio to form the aqueous complex. The solution was kept in dark overnight at room temperature under gentle stirring. The presence of AgCl precipitates confirmed the reaction (8,15,16). Next, centrifugation of the reaction mixture at 10,000 rpm for 10 min and supernatant filtration over 0.22 µm filters was made in order to eliminate AgCl precipitates.

A first attempt consisting of encapsulating the aqueous soluble poly(glutamic acid)-cisplatin complex (PGlu-CDDP) in PBLG-bnz nanoparticles was tested (SM). A second approach consisting of complexing aqueous cisplatin to the carboxylate groups of the preformed PBLG-*b*-PGlu nanoparticles was investigated. The kinetics of the reaction of cisplatin with PBLG-*b*-PGlu nanoparticles at a [CDDP/COO^-] ratio of 1.25 was studied. A purification step by dialysis with a SpectraPor membrane (molecular weight cut off 3000 Da) was performed during 24 h. Secondly, PBLG-*b*-PGlu nanoparticles at a [COO^-] of 0.86 mM were incubated under gentle stirring with the cisplatin aqueous complex solution at different [CDDP/ COO^-] feed ratios ranging from 0 to 1.56 and reacted for 60 h in dark to form the complex between the hydrophilic chains of PGlu and CDDP and purification as described above. Drug loading content (mg of loaded cisplatin/mg of nanoparticles * 100) and association efficiency (mg of loaded cisplatin/mg of initial cisplatin * 100) were expressed in percentage.

In Vitro Cisplatin Release Kinetics

In vitro cisplatin release from the cisplatin-loaded PBLG-*b*-PGlu nanoparticles was studied by the dialysis method in a 0.01 M phosphate buffer saline (PBS pH 7.4) containing 0.138 M of NaCl and in distilled MilliQ water at 37°C. Briefly, 0.950 mL of a PBLG-*b*-PGlu nanoparticle suspension at a concentration of 0.75 mg/mL and containing 0.1% of poloxamer (Pluronic® F68, BASF) were introduced in the 1 mL microdialyzers and dialyzed against 15 mL of medium using dialysis membranes with a molecular weight cut off of 3500 Da. The solution outside the microdialyzers was sampled at defined periods and replaced with fresh medium. Experiments were carried out by triplicate. Control release experiments with a cisplatin solution in the conditions described above were also carried out.

In Vitro Hydroxyapatite (HAP) Binding Assay

Multifunctional nanoparticles containing the fluorescent PBLG-dansyl polymer and the osteotropic PBLG-*b*-PGlu copolymer, loaded with cisplatin at a ratio [CDDP]/[COO^-] = 1.25 and containing 0.1% of poloxamer were incubated in a HAP suspension in PBS (0.4 g/mL) at pH 7.4 at 25°C during 24 h. The suspensions were centrifuged at 5000 rpm for 5 min, washed three times with poloxamer 1% in PBS 7.4 and observed under UV light at 365 nm. Supernatants were quantified by a Perkin Elmer Luminescence spectrometer LS 50B at room temperature ($\lambda_{exCitation} = 340$ nm. $\lambda_{emission} = 472$ nm) so as to determine the amount of nanoparticles not bound to HAP.

Interaction of Cisplatin Released from PBLG-*b*-PGlu Nanoparticles With DNA

Two mL of a cisplatin loaded PBLG-*b*-PGlu nanoparticle suspension at a concentration of 1.5 mg/mL were incubated in PBS (pH 7.4) during 1 week in the presence of an excess of double stranded DNA (dsDNA). A positive control was performed with a 0.2 mM cisplatin solution. Electrochemical experiments were performed at 298 ± 1 K in a thermostated cell with a CH I660 equipment. A BAS MF2012 glassy carbon working electrode (GCE) (geometrical area 0.071 cm^2), a platinum wire auxiliary electrode and an Ag/AgCl (3 M NaCl) reference electrode were used in a conventional three-electrode arrangement. 0.10 M potassium phosphate buffer (pH 7.0) and PBS (pH 7.4), deaerated by argon bubbling during 15 min, were used as supporting electrolytes.

In Vitro Cytotoxicity Studies

The cytotoxic effect of free cisplatin, PBLG-*b*-PGlu nanoparticles and cisplatin-loaded PBLG-*b*-PGlu nanoparticles was studied in three different prostate cancer cell lines: PC-3, DU-145 and LNCaP by the MTS cell viability assay 48 and 72 h after exposure. PC-3, DU-145 and LNCaP were grown in RPMI 1640 (BE 12–702 F, Lonza) supplemented with 10% (*v*/*v*) heat-inactivated fetal bovine serum (Lonza), penicillin (100 UI/mL), and streptomycin (100 µg/mL). Cells were maintained in a 95% humidified atmosphere of 5% CO_2 at 37°C. Cells were seeded in 96-well plates (5.5 10^3 cells per well) and were pre-incubated during 48 h. Then, cisplatin, PBLG-*b*-PGlu nanoparticles and cisplatin-loaded PBLG-*b*-PGlu nanoparticles at different concentrations were added and after 48 or 72 h 20 µL of MTS solution per well were added. Viable cells were quantified by recording the UV absorbance at 492 nm using a plate reader multi-well scanning spectrophotometer (Labsystems Multiskan MS). Cytotoxicity was also followed by the blue trypan exclusion assay. Briefly, fresh media was replaced by trypsin 0.25% EDTA and once cells were in suspension trypan blue was added. Cells were counted through a hemocytometer (Kova slides).

RESULTS

Synthesis and Characterization of PBLG-*b*-PGlu Copolymer

A two step procedure has been successfully used to prepare a PBLG-*b*-PGlu copolymer. First, a PGlu block has been prepared, which in turn has been used as a macroinitiator for the synthesis of the hydrophobic PBLG block. Hexylamine was used to initiate the ROP of BLG-NCA for the synthesis of

hexyl-PBLG polymer. Characteristic ^{1}H NMR peaks were identified and its degree of polymerization (DP_n) was found to be 16 (see SM). Next, debenzylation reaction was driven to completion as confirmed by the absence of the benzyl and aromatic protons peaks in the ^{1}H NMR spectrum of the PGlu polymer (see SM). ^{1}H NMR spectrum of the PBLG-*b*-PGlu copolymer showed characteristics peaks for this copolymer and its molecular weight was determined by SEC (Table I).

Infrared study revealed that the major conformation of PGlu polymer was α-helices, with a minor existence of β-sheets, evidenced by a shoulder at 1628 cm^{-1} (SM) in coherence with the reported secondary structures for PBLG polymers with a DP_n <18 (17) and for PGlu oligomers (18). Carboxylic acids from PGlu were in the protonated state as evidenced by the band at 1710 cm^{-1}. PBLG-*b*-PGlu copolymer presented an α-helix structure, as shown by the amide I amide II and amide III bands at ~1655 cm^{-1}, ~1550 cm^{-1} and ~1260 cm^{-1}, respectively and the ester C=O band at ~1735 cm^{-1} (see SM) (19–21).

PBLG-*b*-PGlu Nanoparticles: Preparation and Cisplatin Association

Novel PBLG-*b*-PGlu nanoparticles (a schematic illustration is shown in Fig. 1), were prepared by a new nanoprecipitation method, modified from a previous one (19). The use of NaOH was essential for nanoparticle preparation since ionization of the carboxylate groups in the hydrophilic PGlu block was necessary to avoid nanoparticle aggregation (SM, figure S7). As shown in Table II, DLS measurements suggested that nanoparticles had a hydrodynamic diameter in the range of 50 nm and a very negative ζ potential. Accurate size measurements from TEM images revealed that they had an ellipsoidal shape with an aspect ratio of 1.3 and an actual size of 37± 7 nm×27±6 nm, with no significant changes in the morphology and size after cisplatin coordination.

As shown in Fig. 2a, the incorporated ratio increased almost linearly when the [CDDP]/[COO^-] feed ratio increased from 0.6 to 1.6, suggesting that no saturation occurred in this range of concentration ratios. The incorporated ratio of 0.27, where free ionized COO^- groups not coordinated to cisplatin remained, was considered to be a good balance between cisplatin loading and nanoparticle stability (up to several months without aggregation or precipitation behaviour). Therefore, a [CDDP]/[COO^-] feed ratio of 1.25 was chosen for further experiments. At this feed ratio, drug loading content was found to be 6.2±0.23% (*w*/*w*) with a drug association efficacy of 16±0.58% (*w*/*w*). As shown in Fig. 2b, the kinetics of the reaction of the carboxylates on the outer shell of the PBLG-*b*-PGlu nanoparticles and aqueous cisplatin was almost completed in 3 h, consistently with previous works (22).

Table I Experimental Molecular Weights of the PBLG Polymers Determined by SEC

PBLG polymers	M_n (g/mol)	PI
PBLG-*b*-PGlu	24436	1.7
PBLG-bnz	31727	1.1
PBLG-dansyl	25944	1.1

PBLG-*b*-PGlu Nanoparticle Interaction with Cisplatin by ITC

ITC experiments were conducted to study the interaction between PBLG-*b*-PGlu nanoparticles and cisplatin. An interaction was found that did not exist for the negative control PBLG-bnz nanoparticles (Fig. 3), considered as the core of the PBLG-*b*-PGlu nanoparticles. The effect of 2 equivalents of NaOH used during nanoparticle preparation on the cisplatin association was found to be negligible.

Heats measured in ITC experiments are the sum of different processes implied during cisplatin association to nanoparticles, including the PGlu block conformation changes (23). Cisplatin contains two chloride ligands that can be replaced by the carboxylate groups belonging to the PBLG-*b*-PGlu nanoparticle shells. At low [CDDP]/[COO^-] ratios, as in the conditions of the experiment, a stoichiometry of two COO^- per CDDP was favoured. Carboxylate-metal complexes could occur between cisplatin and carboxylate groups belonging to the same or an adjacent PGlu chain, inducing conformational changes that could induce heat variations. Therefore, the heat measured included both cisplatin binding to the carboxylate groups and possible conformation changes of the PGlu chains induced by it.

In Vitro Cisplatin Release Kinetics

As shown in Fig. 4, in presence of chloride ions, cisplatin-loaded PBLG-*b*-PGlu nanoparticles released cisplatin in a sustained manner with a remarkable absence of any initial burst under physiological conditions. The absence of a burst effect suggests that cisplatin was mainly associated to nanoparticles through complexation to the carboxylate groups and not physically entrapped. An almost linear release profile was obtained suggesting an almost zero order kinetics in the whole range. Cisplatin release from nanoparticles in PBS was slow; less than 10 and 50% of cisplatin was released after 24 h and 7 days, respectively. Remarkably, cisplatin was completely released from the PBLG-*b*-PGlu nanoparticles, more than 90% was released after 14 days. Release of cisplatin in distilled water medium did take place, contrarily to previous works with cisplatin-carboxylate complexes (8,15,16) and micelles (22,24), although it was considerably reduced, since less than 2% and only 20% of the initial dose was released after 48 h and 14 days respectively. It cannot be excluded that the release in water could be due to the slightly mild acid pH of

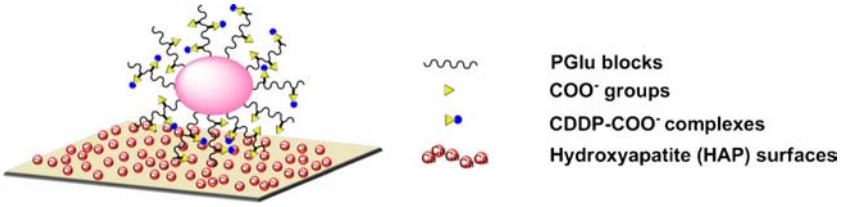

Fig. 1 Schematic illustration of PBLG-*b*-PGlu nanoparticles showing their simultaneous dual functionality. Nanoparticles show core-shell structure where the hydrophobic core (in *pink*) is formed by the self-assembly of the rigid PBLG blocks where as the hydrophilic shell is formed by the PGlu blocks. The carboxylate groups (COO^-) belonging to the hydrophilic blocks PGlu provide nanoparticles with both hydroxyapatite targeting and anticancer properties provided by cisplatin binding and release.

distilled water (pH around 6.8), in coherence with previous works (25).

In Vitro HAP Binding Assay

The *in vitro* HAP binding kinetics assay showed a total binding for fluorescently labelled blank and cisplatin-loaded PBLG-*b*-PGlu nanoparticles (33% of PBLG-dansyl and 66% of PBLG-*b*-PGlu) (Fig. 5a) in contrast to the absence of binding for 100% PBLG-dansyl nanoparticles. It also revealed a slightly fastened binding for the cisplatin-loaded PBLG-*b*-PGlu nanoparticles compared to the blank ones. The HAP desorption assay at acidic pH revealed a differential binding for these two types of PBLG-*b*-PGlu nanoparticles (cisplatin loaded and the corresponding blank ones). For both types of nanoparticles, no desorption occurred at pH 5.5 and pH 4.5. For blank PBLG-*b*-PGlu nanoparticles desorption was total at pH 3.5 whereas for the cisplatin-loaded ones the percentage of desorbed nanoparticles was of 40%.

Interaction of Cisplatin Released from PBLG-*b*-PGlu Nanoparticles With DNA

An electrochemical technique has been used to assess the capability of platinum species to interact with DNA after being progressively released from cisplatin-loaded PBLG-*b*-PGlu nanoparticles. Indeed, electrochemical detection techniques can be conveniently used to monitor cisplatin interactions with DNA (26). Voltammograms for cisplatin-loaded PBLG-*b*-PGlu nanoparticles incubated with PBS in presence or absence of a DNA solution were different (Fig. 6). The response of free cisplatin with DNA in phosphate buffer was considered as a positive control. The voltammograms showed intense peaks at −1.10 V, corresponding to the interaction of free cisplatin with DNA. The peak observed at −0.45 V in the case of free cisplatin (Fig. 6a and b) could be attributed to the adsorption of cisplatin to the electrode surface. Further voltamogramms in Fig. 6c and d suggested that the cisplatin released from the cisplatin-loaded PBLG-*b*-PGlu nanoparticles during PBS incubation was able to interact with the DNA strands similarly to free cisplatin.

In Vitro Cytotoxicity Assay

The MTS assay revealed that PBLG-*b*-PGlu nanoparticles exhibited no or very low toxicity for PC-3 and DU 145 cell lines whereas for LNCaP cell line they were not toxic under 25 μM (SM). It showed a dose-dependent response on all three cell lines (Table III). IC_{50} values for cisplatin-loaded PBLG-*b*-PGlu nanoparticles were 6–15 times higher than for free cisplatin evidencing a lower cytotoxicity for nanoparticles, which was also confirmed by the blue trypan assay (SM).

Table II Size and ζ Potential Determined by DLS of PBLG-Derivate and PBLG-b-PGlu Nanoparticles Prepared at Different [CDDP]/[COO-] Ratios

Nanoparticles	Size (nm) ± SD [a]	Polydispersity Index ± SD [a]	ζ Potential (meV) ± SD [a]	Drug loading content [b] (*w/w*%)
PBLG-bnz	57 ± 1.1	0.17 ± 0.073	−37 ± 2.5	0
PBLG-dansyl	58 ± 0.91	0.12 ± 0.0077	−45 ± 1.5	0
PBLG-*b*-PGlu	53 ± 0.11	0.13 ± 0.010	−37 ± 2.4	0
After CDDP loading at [CDDP]/[COO^-] ratio of:				
0.3	52 ± 0.61	0.22 ± 0.075	−36 ± 2.5	0.36
0.5	49 ± 1.1	0.15 ± 0.049	−34 ± 0.3	0.62
0.8	49 ± 0.12	0.17 ± 0.0071	−34 ± 0.81	2.3
1.0	51 ± 0.53	0.12 ± 0.0089	−32 ± 2.2	5.3
1.2	50 ± 0.31	0.12 ± 0.0077	−35 ± 0.74	5.9
1.6	51 ± 0.33	0.15 ± 0.0084	−33 ± 1.3	8.3

[a] ($n = 3$); [b] CDDP content determined by AAS expressed as mass of associated CDDP per mass of nanoparticles (% *w/w*)

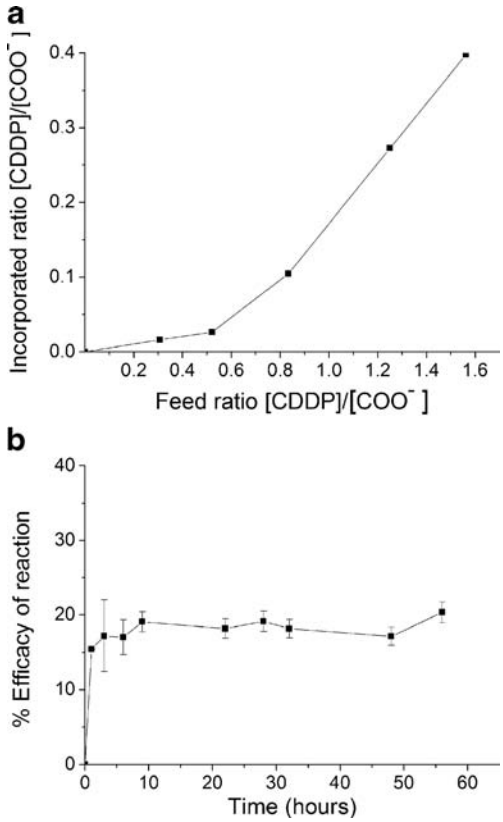

Fig. 2 Cisplatin association to PBLG-PGlu nanoparticles. (**a**) [CDDP]/[COO^-] incorporated ratio to the PBLG-*b*-PGlu nanoparticles at different [CDDP]/[COO^-] feed ratios (**b**) Kinetics of the reaction of PBLG-*b*-PGlu nanoparticles with aqueous cisplatin at a [CDDP]/[COO^-] ratio of 1.25.

This might be related to the fact that cisplatin is coordinated to PBLG-*b*-PGlu nanoparticles and is slowly released. Cytotoxicity of cisplatin-loaded PBLG-*b*-PGlu nanoparticles appeared to be enhanced with time as suggested by the 48 and

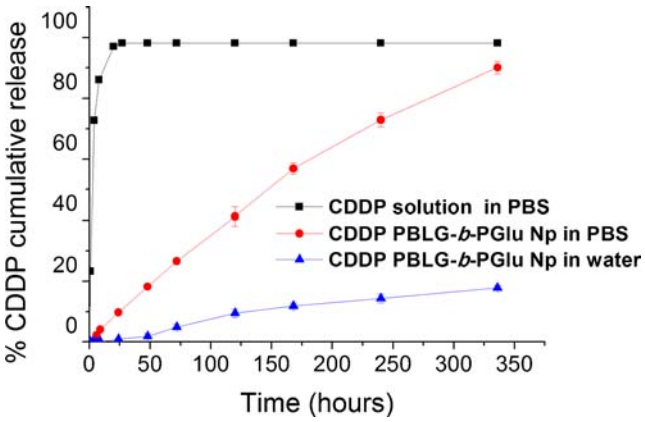

Fig. 4 *In vitro* cisplatin release from a cisplatin solution (*black square*), from cisplatin-loaded PBLG-*b*-PGlu nanoparticles in 0.01 M PBS (pH 7.4) containing 0.138 M of NaCl (*red circle*) and in water (*blue triangle*).

72 h IC_{50} values. This suggests the need for an elapsed time for nanoparticles to be cytotoxic either through metastatic cell internalisation or cisplatin release in their vicinity.

DISCUSSION

Nanoparticles with enhanced residence time within the bone could constitute a valuable strategy for the treatment of bone cancers. In this view, PBLG-*b*-PGlu, which was synthesised by a living polymerization, was shown to easily assemble into nanoparticles. These nanoparticles showed for the first time dual hydroxyapatite binding and anticancer properties mediated by the PGlu moiety. The use of the single copolymer PBLG-*b*-PGlu to provide both functionalities enables a simple

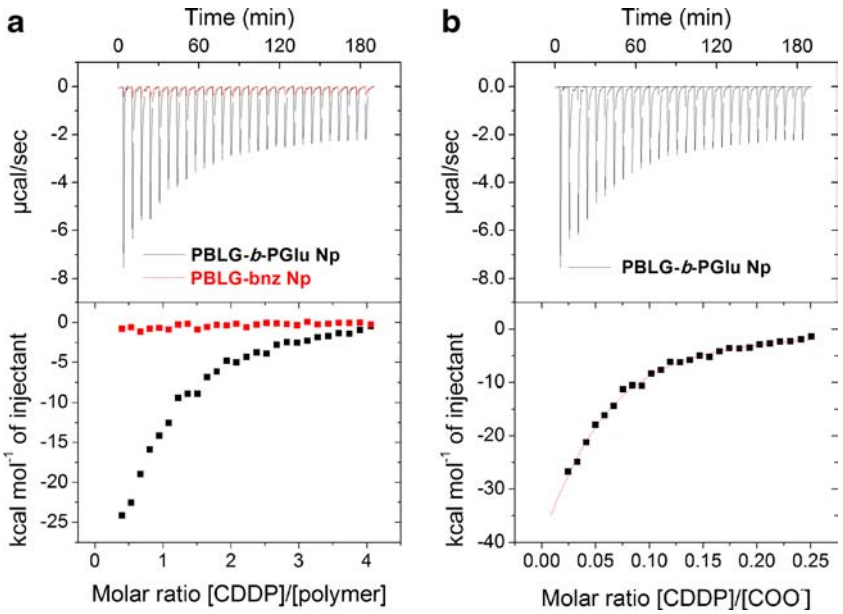

Fig. 3 Typical ITC raw data and integrated heat data profiles obtained from the interaction of cisplatin at 0.8 mM with PBLG-*b*-PGlu nanoparticles at [polymer] of 0.042 mM compared to the negative control PBLG-bnz nanoparticles (**a**) and at [COO^-] of 0.68 mM (**b**).

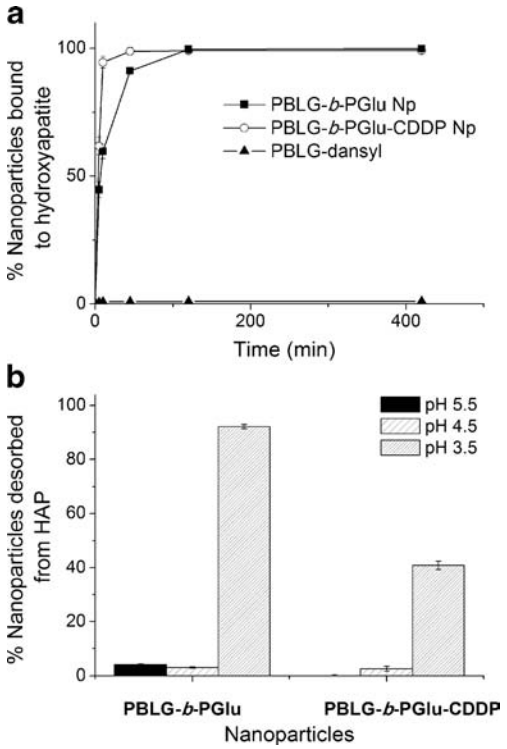

Fig. 5 (**a**) Binding kinetics expressed in percentage of nanoparticles bound to HAP ($n=3$). Nanoparticles at a concentration of 1.5 mg/mL in 0.1% poloxamer were incubated with 0.4 g of HAP suspension in PBS. (**b**) Desorption of the different HAP-bound nanoparticles at the following consecutive pH: 5.5, 4.5 and 3.5 ($n=3$)

pharmacotechnical nanoparticle preparation in view of an easy scale-up. Nanoparticles presented an oblate form with a longitudinal diameter smaller than 40 nm. They might exhibit a core-shell structure, where the inner hydrophobic core is formed by the stacking of rigid α-helices of the PBLG blocks and the outer shell by the hydrophilic PGlu chains. PGlu chain conformation is known to be dependent on pH. At acidic pH (<4.3–4.9) the PGlu chains are protonated (27) and can adopt an α-helix conformation whereas when side chains are electrically charged (pH>5), electrostatic repulsion between them induces a random coil conformation (28–30). At the pH of nanoparticle suspensions (7.9), carboxylate groups were ionized and thus PGlu might adopt a random coil conformation forming an outer hydrophilic flexible shell.

Once PBLG-*b*-PGlu colloidal suspensions were obtained, cisplatin was associated to the preformed PBLG-*b*-PGlu nanoparticles through incubation with an aqueous cisplatin solution, which is most appropriate for complex formation due to better leaving group properties of hydroxide/water molecules compared to chloride ions. Association of cisplatin to nanoparticles might have an impact on the nanoparticle structure, as evidenced by ITC experiments. Cisplatin coordination to some of the carboxylic groups belonging to the PGlu block could decrease PGlu hydrophilicity, consistently with previous works (22). This

Table III IC_{50} Values for Free Cisplatin and Cisplatin-Loaded PBLG-*b*-PGlu Nanoparticles After 48 and 72 h After Exposure Determined by the MTS Assay

Cell line		IC_{50} (μM) 48 h	IC_{50} (μM) 72 h
PC-3	Cisplatin	8.7	7.8
	Cisplatin -PBLG-*b*-PGlu np	25	13
DU-145	Cisplatin	5.8	2.6
	Cisplatin-PBLG-*b*-PGlu np	>35	26
LNCaP	Cisplatin	2.3	1.7
	Cisplatin -PBLG-*b*-PGlu np	24	4.8

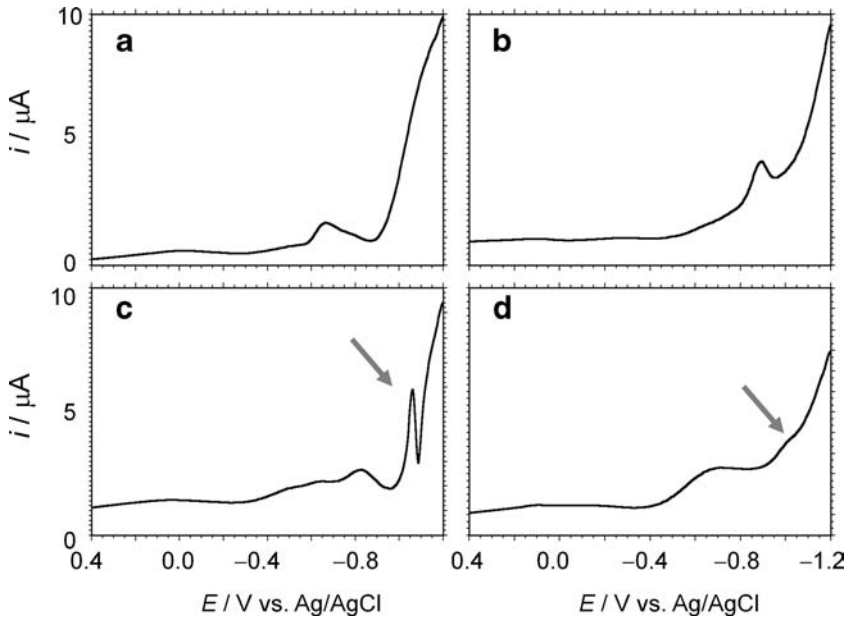

Fig. 6 Square wave voltammetry (SWVs) for (**a**) cisplatin solution in phosphate buffer (pH 7.0); (**b**) cisplatin-loaded PBLG-*b*-PGlu nanoparticles in phosphate buffer; (**c**) free cisplatin diluted in PBS (pH 7.4) and incubated with DNA for 24 h (**d**) cisplatin loaded PBLG-*b*-PGlu nanoparticles previously incubated in PBS for 5 days and with DNA for 24 hours. Potential scan initiated at +0.4 V in the negative direction; potential step increment 4 mV; square wave amplitude 25 mV; frequency 5 Hz. *Arrows* indicate the DNA-bound cisplatin signal

could hypothetically result in the formation of hydrophobic microdomains that would fold onto the hydrophobic nanoparticle core surface while some hydrophilic domains of the PGlu chains would expand out of the surface.

In order to provide nanoparticles with anticancer properties, cisplatin was selected since it is clinically used for metastatic prostate cancer. Several approaches were tested in order to obtain adequate cisplatin content and controlled release kinetics compatible with the potential application of prolonged time of residence within the bone. Since cisplatin is a water soluble and hydrophilic molecule, direct cisplatin encapsulation into the PBLG nanoparticles was not considered. Cisplatin-PGlu encapsulation into PBLG-bnz nanoparticles was found to be negligible in spite of the structural similarity between PGlu and PBLG-bnz (SM). The approach consisting of complexing cisplatin to the carboxylate groups of preformed PBLG-*b*-PGlu nanoparticles allowed higher drug loading contents and an almost zero controlled kinetics during 14 days, triggered by physiological concentrations of chloride ions.

Cisplatin has two chloride groups that can be replaced by a variety of groups, such as carboxylates in low chloride concentration medium. The good leaving property of carboxylates makes the metal complex reversible, such property being used for the design of drug carrier systems (8,16,22,24,31). In coherence with previous works, the presence of chloride ions is essential for cisplatin release due to a ligand exchange reaction where chloride ions would substitute the Glu residues from the PBLG-*b*-PGlu nanoparticle (22). Other ions such as acetates or phosphates can also play a minor role in the release of cisplatin. An enhanced cisplatin release from carboxylate complex at mild acidic pH has also been reported (25). The initial ratio [CDDP/COO^-] was adjusted to 1.25 to have an optimal balance between stability and cisplatin association. Kinetics of association was found to be very rapid (~3 h) in contrast to the controlled cisplatin release (~14 days). These differences can be attributed to the fact that cisplatin association to PGlu and cisplatin release in presence of chloride ions are two distinct chemical reactions.

In order to study HAP binding properties, nanoparticles were provided with fluorescent properties (PBLG-dansyl) thanks to the versatile nanoprecipitation method, which allowed the preparation of nanoparticles from mixtures of PBLG polymers (32). Cisplatin PBLG-*b*-PGlu nanoparticles were shown to bind effectively to HAP. Indeed, oligomers of glutamic acid have been shown to have both *in vitro* and *in vivo* affinity to bone matrix and HAP, respectively (6) and they have been used to provide drugs with osteotropic properties (33). Interestingly, the complexation of cisplatin to PBLG-*b*-PGlu nanoparticles at a [CDDP]/[COO^-] ratio of 1.25 did not alter their degree of HAP binding. Both the *in vitro* HAP binding kinetics and desorption at acidic pH suggested that not only the remaining free carboxylate groups but also the cisplatin itself were involved in the binding to HAP, in coherence with previously works (34).

Adduct formation between DNA and platinum derivates is one of the mechanisms responsible for their cytotoxicity. Interestingly, an electrochemical method allowed to confirm the interaction of cisplatin released from PBLG-*b*-PGlu nanoparticles with the dsDNA. Consistently, cisplatin-loaded PBLG-*b*-PGlu nanoparticles were shown to be cytotoxic in three different prostate cancer cell lines that have the potential to metastasize to bone [14]. Their cytotoxicity was lower than that of free cisplatin, as already reported for other cisplatin carboxylate coordination complexes within a wide range of cancer cell lines, where it did not compromise the antitumour activity [11, 28]. Once distributed to bone and thanks to their bone binding properties PBLG-*b*-PGlu nanoparticles could remain for a prolonged time in the bone tumour vicinity, and thus they could constitute drug reservoirs for sustained cisplatin release in view of the treatment of skeletal malignancies.

CONCLUSION

We report the simple preparation of novel PBLG-*b*-PGlu nanoparticles with the dual functionality of hydroxyapatite binding and efficient cisplatin loading and controlled release. PBLG-*b*-PGlu nanoparticles could complex cisplatin at a payloads of 6.2% (*w*/*w*) and released it in a very sustained way, triggered by chloride ions, in order to produce cytotoxic effects in three different prostate cancer cell lines that could potentially metastasize to bone.

Simultaneously, cisplatin-loaded PBLG-*b*-PGlu nanoparticles showed very efficient *in vitro* hydroxyapatite binding. Favourably, chloride triggered sustained cisplatin release from these nanoparticles may help to prolong cytotoxic effects, making them promising carriers for the treatment of bone metastases.

ACKNOWLEDGMENTS AND DISCLOSURES

We gratefully acknowledge the European postgraduate program from "Ibercaja Foundation" for the financial support of Laura de Miguel. This work has benefited from the facilities and expertise of the Platform for Transmission Electronic Microscopy of IMAGIF (Centre de Recherche de Gif - www.imagif.cnrs.fr) and we thank Miss Cynthia Gillet for her valuable help with the TEM image acquisitions. We thank Dr Silvia Mazzaferro and LCPO, Univ. Bordeaux, CNRS, UMR 5629 for the SEC analyses.

REFERENCES

1. Siegel R, Naishadham D, Jemal A. Cancer statistics. CA Cancer J Clin. 2012;62(1):10–29.

2. Coleman RE. Metastatic bone disease: clinical features, pathophysiology and treatment strategies. Cancer Treat Rev. 2001;27(3):165–76.
3. Hirabayashi H, Fujisaki J. Bone-specific drug delivery systems: approaches via chemical modification of bone-seeking agents. Clin Pharmacokinet. 2003;42(15):1319–30.
4. Low SA, Kopeček J. Targeting polymer therapeutics to bone. Adv Drug Deliv Rev. 2012;64(12):1189–204.
5. Fujisaki J, Tokunaga Y, Takahashi T, Kimura S, Shimojo F, Hata T. Osteotropic drug delivery system (ODDS) based on bisphosphonic prodrug. V. Biological disposition and targeting characteristics of osteotropic estradiol. Biol Pharm Bull. 1997;20(11):1183–7.
6. Sekido T, Sakura N, Higashi Y, Miya K, Nitta Y, Nomura M, *et al.* Novel drug delivery system to bone using acidic oligopeptide: pharmacokinetic characteristics and pharmacological potential. J Drug Target. 2001;9(2):111–21.
7. Kasugai S, Fujisawa R, Waki Y, Miyamoto K, Ohya K. Selective drug delivery system to bone: small peptide (Asp)6 conjugation. J Bone Miner Res. 2000;15(5):936–43.
8. Ye H, Jin L, Hu R, Yi Z, Li J, Wu Y, *et al.* Poly(gamma-L-glutamic acid) cisplatin conjugate effectively inhibits human breast tumor xenografted in nude mice. Biomaterials. 2006;27(35):5958–65.
9. Pinzani V, Bressolle F, Johanne Haug I, Galtier M, Blayac JP, Balmès P. Cisplatin-induced renal toxicity and toxicity-modulating strategies: a review. Cancer Chemother Pharmacol. 1994;35(1):1–9.
10. Harmers FP, Gispen WH, Neijt JP. Neurotoxic side-effects of cisplatin. Eur J Cancer. 1991;27(3):372–6.
11. Galanski M, Keppler BK. Searching for the magic bullet: anticancer platinum drugs which can be accumulated or activated in the tumor tissue. Anticancer Agents Med Chem. 2007;7(1):55–73.
12. Yonou H, Yokose T, Kamijo T, Kanomata N, Hasebe T, Nagai K, *et al.* Establishment of a novel species- and tissue-specific metastasis model of human prostate cancer in humanized non-obese diabetic/severe combined immunodeficient mice engrafted with human adult lung and bone. Cancer Res. 2001;61(5):2177–82.
13. Higashi N, Koga T, Niwa M. Helical superstructures from a poly(γ-benzyl-l-glutamate)−poly(l-glutamic acid) amphiphilic diblock copolymer: monolayer formation on water and its specific binding of amino acids. Langmuir. 2000;16(7):3482–6.
14. Crespo JS, Lecommandoux S, Borsali R, Klok HA, Soldi V. Small-angle neutron scattering from diblock copolymer poly(styrene-d_8)-b-poly(γ-benzyl l-glutamate) solutions: rod−coil to coil−coil transition. Macromolecules. 2003;36(4):1253–6.
15. Feng Z, Lai Y, Ye H, Huang J, Xi XG, Wu Z. Poly (gamma- L-glutamic acid)-cisplatin bioconjugate exhibits potent antitumor activity with low toxicity: a comparative study with clinically used platinum derivatives. Cancer Sci. 2010;101(11):2476–82.
16. Zhu W, Li Y, Liu L, Zhang W, Chen Y, Xi F. Biamphiphilic triblock copolymer micelles as a multifunctional platform for anticancer drug delivery. J Biomed Mater Res A. 2010;96A(2):330–40.
17. Papadopoulos P, Floudas G, Klok HA, Schnell I, Pakula T. Self-assembly and dynamics of poly(gamma-benzyl-l-glutamate) peptides. Biomacromolecules. 2004;5(1):81–91.
18. Rinaudo M, Domard A. Circular dichroism studies on alpha-L-glutamic acid oligomers in solution. J Am Chem Soc. 1976;98(20):6360–4.
19. Barbosa MEM, Montembault V, Cammas-Marion S, Ponchel G, Fontaine L. Synthesis and characterization of novel poly(γ-benzyl-L-glutamate) derivatives tailored for the preparation of nanoparticles of pharmaceutical interest. Polym Int. 2007;56(3):317–24.
20. Segura-Sanchez F, Montembault V, Fontaine L, Martinez-Barbosa ME, Bouchemal K, Ponchel G. Synthesis and characterization of functionalized poly(gamma-benzyl-L-glutamate) derivates and corresponding nanoparticles preparation and characterization. Int J Pharm. 2010;387(1–2):244–52.
21. Buffeteau T, Le Calvez E, Castano S, Desbat B, Blaudez D, Dufourcq J. Anisotropic optical constants of α-helix and β-sheet secondary structures in the infrared. J Phys Chem B. 2000;104(18):4537–44.
22. Nishiyama N, Yokoyama M, Aoyagi T, Okano T, Sakurai Y, Kataoka K. Preparation and characterization of self-assembled polymer metal complex micelle from cis-dichlorodiammineplatinum(II) and poly(ethylene glycol)-poly(L-aspartic acid) block copolymer in an aqueous medium. Langmuir. 1999;15(2):377–83.
23. Chou PY, Scheraga HA. Calorimetric measurement of enthalpy change in the isothermal helix–coil transition of poly-L-lysine in aqueous solution. Biopolymers. 1971;10(4):657–80.
24. Nishiyama N, Kataoka K. Preparation and characterization of size-controlled polymeric micelle containing cis-dichlorodiammineplatinum(II) in the core. J Control Release. 2001;74(1–3):83–94.
25. Xia Y, Wang Y, Wang Y, Tu C, Qiu F, Zhu L, *et al.* A tumor pH-responsive complex: Carboxyl-modified hyperbranched polyether and cis-dichlorodiammineplatinum(II). Colloids Surf B: Biointerfaces. 2011;88(2):674–81.
26. Krizkova S, Adam V, Petrlova J, Zitka O, Stejskal K, Zehnalek J, *et al.* A suggestion of electrochemical biosensor for study of platinum(II)-DNA interactions. Electroanalysis. 2007;19(2–3):331–8.
27. Nilsson S, Zhang W. Helix-coil transition of a titrating polyelectrolyte analyzed within the Poisson-Boltzmann cell model: effects of pH and salt concentration. Macromolecules. 1990;23(25):5234–9.
28. Olander DS, Holtzer A. Stability of the polyglutamic acid alpha helix. J Am Chem Soc. 1968;90(17):4549–60.
29. Holtzer A, Hawkins RB. The state of aggregation of α-helical poly(l-glutamic acid) in aqueous salt solutions. J Am Chem Soc. 1996;118(17):4220–1.
30. Kimura T, Takahashi S, Akiyama S, Uzawa T, Ishimori K, Morishima I. Direct observation of the multistep helix formation of poly-l-glutamic acids. J Am Chem Soc. 2002;124(39):11596–7.
31. Gianasi E, Wasil M, Evagorou EG, Keddle A, Wilson G, Duncan R. HPMA copolymer platinates as novel antitumour agents: in vitro properties, pharmacokinetics and antitumour activity in vivo. Eur J Cancer. 1999;35(6):994–1002.
32. de Miguel L, Noiray M, Surpateanu G, Iorga BI, Ponchel G. Poly(γ-benzyl-L-glutamate)-PEG-alendronate multivalent nanoparticles for bone targeting. Int J Pharm. 2014;460(1–2):73–82.
33. Ishizaki J, Waki Y, Takahashi-Nishioka T, Yokogawa K, Miyamoto K-I. Selective drug delivery to bone using acidic oligopeptides. J Bone Miner Metab. 2009;27(1):1–8.
34. Barroug A, Glimcher MJ. Hydroxyapatite crystals as a local delivery system for cisplatin: adsorption and release of cisplatin in vitro. J Orthop Res. 2002;20(2):274–80.